Chemistry Europe
European Chemical Societies Publishing

WILEY VCH

Excellence in Chemistry Research

Announcing our new flagship journal

- Gold Open Access
- Publishing charges waived
- Preprints welcome
- Edited by active scientists

Meet the Editors of *ChemistryEurope*

Luisa De Cola
Università degli Studi di Milano Statale, Italy

Ive Hermans
University of Wisconsin-Madison, USA

Ken Tanaka
Tokyo Institute of Technology, Japan

Chemistry–A European Journal
Research Article
doi.org/10.1002/chem.202300540
Chemistry Europe
European Chemical Societies Publishing
www.chemeurj.org

Development of Fluorescent Isocoumarin-Fused Oxacyclononyne – 1,2,3-Triazole Pairs

Aleksandra A. Vidyakina,[a] Andrey A. Shtyrov,[b] Mikhail N. Ryazantsev,[a, b] Alexander F. Khlebnikov,[a] Ilya E. Kolesnikov,[a] Vladimir V. Sharoyko,[a] Dar'ya V. Spiridonova,[a] Irina A. Balova,[a] Stefan Bräse,*[c, d] and Natalia A. Danilkina*[a]

Dedicated to the 300th anniversary of the Saint Petersburg University foundation.

Abstract: Fluorescent isocoumarin-fused cycloalkynes, which are reactive in SPAAC and give fluorescent triazoles regardless of the azide nature, have been developed. The key structural feature that converts the non-fluorescent cycloalkyne/triazole pair to its fluorescent counterpart is the pi-acceptor group (COOMe, CN) at the C6 position of the isocoumarin ring. The design of the fluorescent cycloalkyne/triazole pairs is based on the theoretical study of the S1 state deactivation mechanism of the non-fluorescent isocoumarin-fused cycloalkyne **IC9O** using multi-configurational ab initio and DFT methodologies. The calculations revealed that deactivation proceeds through the electrocyclic ring opening of the α-pyrone cycle and is accompanied by a redistribution of electron density in the fused benzene ring. We proposed that the S1 excited state deactivation barrier could be increased by introducing a pi-acceptor group into a position that is in direct conjugation with the formed C=O group and has a reduced electron density in the transition state. As a proof of concept, we designed and synthesized two fluorescent isocoumarin-fused cycloalkynes **IC9O-COOMe** and **IC9O-CN** bearing pi-acceptors at the C6 position. The importance of the nature of a pi-acceptor group was shown by the example of much less fluorescent CF_3-substituted cycloalkyne **IC9O-CF_3**.

Introduction

Bioconjugation through bioorthogonal click reactions is an indispensable tool in chemistry and biology, which allows the modification of various biomolecules selectively under mild conditions, both outside and inside living cells and organisms.[1–9] The invaluable role of bioorthogonal click chemistry, discovered by Carolyn Bertozzi, was recognizes with a Nobel Prize in 2022.[10] Strain-promoted azide–alkyne cycloadditions (SPAAC),[11] that is, the reaction between a bioorthogonal azido group and a bent alkyne moiety is one of the most important tools for bioorthogonal bioconjugation.[12–15]

The crucial role of SPAAC is determined by the unique properties of the azido group,[16] fast SPAAC kinetics, and a wide range of available cycloalkyne-based reagents.[17–27]

Nevertheless, to use SPAAC to visualize modified biomolecules, a cycloalkyne reagent should be preconjugated with a fluorescent dye which introduces an additional synthetic, structural, and functional load.[28] In this regard, the design and synthesis of cycloalkynes which give fluorescent triazoles, would enable the avoidance of additional synthetic steps and undesirable structural complexity.

To achieve this end, the cycloalkyne must be either fluorogenic or fluorescent on its own and retain its fluorescence in SPAAC products. However, only a few examples of fluorogenic SPAAC reagents have been reported (Figure 1). The

[a] A. A. Vidyakina, Dr. M. N. Ryazantsev, Prof. Dr. A. F. Khlebnikov, Dr. I. E. Kolesnikov, Dr. V. V. Sharoyko, Dr. D.'y. V. Spiridonova, Prof. Dr. I. A. Balova, Dr. N. A. Danilkina
Institute of Chemistry
Saint Petersburg State University (SPbU)
Sankt-Peterburg, 199034 Saint Petersburg (Russia)
E-mail: n.danikina@spbu.ru

[b] A. A. Shtyrov, Dr. M. N. Ryazantsev
Nanotechnology Research and Education Centre RAS
Saint Petersburg Academic University
Sankt-Peterburg, 194021 Saint Petersburg (Russia)

[c] Prof. Dr. S. Bräse
Institute of Organic Chemistry (IOC)
Karlsruhe Institute of Technology (KIT)
76131 Karlsruhe (Germany)
E-mail: stefan.braese@kit.edu

[d] Prof. Dr. S. Bräse
Institute of Biological and Chemical Systems – Functional Molecular Systems (IBCS-FMS)
Karlsruhe Institute of Technology (KIT)
76344 Eggenstein-Leopoldshafen (Germany)

Supporting information for this article is available on the WWW under https://doi.org/10.1002/chem.202300540

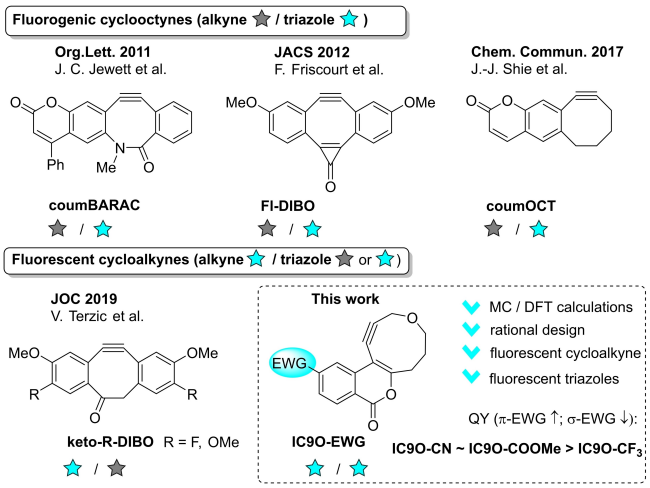

Figure 1. Known examples of fluorogenic/fluorescent cyclooctynes and the fluorescent cycloalkynes **IC9O-EWG** developed in the current work.

annulation of a cyclooctyne core with a known fluorochromic heterocycle, coumarin, led to fluorogenic cyclooctynes **coumBARAC**[29] and **coumOCT**.[30] **FI-DIBO**[31] is another fluorogenic cyclooctyne that belongs to the dibenzocyclooctynes family and shows improved photophysical properties compared with **coumBARAC** and **coumOCT**. It is noteworthy that only in the case of **FI-DIBO** a detailed theoretical explanation of the fluorogenic properties was given. On the other hand, known fluorescent derivatives of **keto-DIBO** lost their ability to fluoresce after conversion to triazoles.[32] Consequently, the discovery of fluorescent cycloalkyne/triazole pairs would help to expand the range of available SPAAC reagents that do not require additional conjugation with a dye.

It is possible to develop a general concept for creating new fluorescent cycloalkyne/triazole pairs based on understanding the mechanism of deactivation of the excited states (ES) of known non-fluorescent cycloalkyne/triazole scaffolds. This can be achieved using computational methods, as well as by predicting and implementing methods for eliminating deactivation pathways. Here we report the applicability of this approach in developing fluorescent SPAAC reagents **IC9O-EWG** (Figure 1).

Results and Discussion

Although fluorescent compounds bearing a coumarin core are important fluorescent dyes,[33,34] isocoumarin-based fluorophores are much less common. Thus, only the naturally-occurring isocoumarin legioliulin[35] responsible for a white-blue fluorescence of *Legionella dumoffii*[36] and several fluorescent isocoumarins useful for sensing various heavy metal ions have been reported.[37–39]

We have recently developed isocoumarin-fused heterocyclononynes as a new type of cycloalkynes, with an interesting interplay of steric factors and stereoelectronic effects responsible for their SPAAC reactivity.[40] However, only the azacyclononyne was dye-modified, resulting in the **IC9N-BDP-FL** reagent. Modification of the more active SPAAC oxacyclononyne **IC9O** with a fluorescent dye could not be achieved due to the lack of the required functionality. On the other hand, synthetically available and stable **IC9O** contains an isocoumarin ring, which is a potential fluorfiophore. Therefore, we chose the non-fluorescent **IC9O**/triazole pair as the focus for this study and turned to calculations to understand the reasons for the lack of fluorescent properties in **IC9O** and explore a way to obtain fluorescent derivatives.

Considering that most bioorthogonal transformations with cycloalkynes are carried out under aqueous conditions, and water is known as a solvent that can either increase or decrease the fluorescence intensity of a probe depending on the mechanism of fluorescence,[41] all calculations were performed in water. Cyclononyne **IC9O** was placed in a 12 Å cubic solvent box (water), and the system was equilibrated by a 10 ns molecular dynamics run (T = 298K, P = 1atm); OPLS force field was used both for solute and solvent at this step. After equilibration, a snapshot closest to the average was extracted and used for further QM/MM calculations, where **IC9O** was treated at the QM level and water molecules at the MM level. Specifically, PBE0/cc-pVDZ/OPLS and MCPDFT(12,12)-tPBE/cc-pVDZ/OPLS[42] levels of theory were employed for the ground state minimum geometry optimization and geometry optimization of critical points on the S1 excited state potential energy surface (S1 min, S1 max, and S1/S0 conical intersection), respectively. NEVPT2(14,13)/cc-pVDZ/OPLS was applied for single-point calculations on optimized geometries (for details, see Supporting Information, Sections 7, 8).

We calculated the absorption band maximum of **IC9O** for a water solution to verify our computational model. The calculated value (λ_{max} = 335 nm) is in excellent agreement with the experiment (λ_{max} = 336 nm; see Figure 2 and Figure 4 below).

To investigate the mechanism of cyclononyne **IC9O** deactivation after the S0→S1 transition, we located critical points on the S0 and S1 potential energy surfaces that govern this process: S0 and S1 minima (S0 min, S1 min) the S1 barrier (transition state barrier, S1 TS) and S0/S1 conical intersection (CI) (Figure 2). An analysis of the **IC9O** molecular structure in the Frank-Condon (FC) region and the CI region revealed that

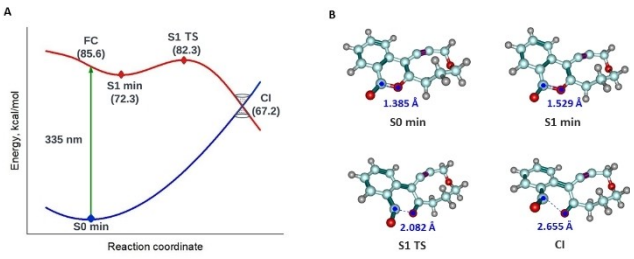

Figure 2. Calculated critical points on S0 (nevpt2(14,13)/cc-pVDZ:OPLS//PBE0/cc-pVDZ:OPLS) and S1 (nevpt2(14,13)/cc-pVDZ:OPLS//MCPDFT(12,12)-tPBE/cc-pVDZ:OPLS) potential energy surfaces for **IC9O** (A) and the corresponding geometries (B). The energies (in kcal/mol) shown in the figure are adiabatic energy differences with respect to the S0 min. Calculated maxima for the absorption band (in nm) corresponds to a vertical transition between S0 and S1 potential energy surfaces.

the main structural change that occurred upon reaching the CI was breaking of the isocoumarin ester bond (Figure 2).

It is known that α-pyrones, isocoumarins, and their thia/thio analogues can undergo photochemical electrocyclic ring opening to form unstable ketenoaldehydes[43–45] or can form dimeric products.[46] Thus, the cleavage of the ester bond found in silico is in good agreement with the known properties of α-pyrones and isocoumarins and can be considered the main reason for the nonradiative deactivation of S1.

It seems quite logical that to eliminate the undesirable deactivation of S1, it would be possible to suggest an increase in the TS barrier from S1 min to the CI. An analysis of the electron density distribution at the FC point and at the S1 TS point reveals that the main factor controlling the energy is the reorganization of the electron density (Scheme 1, see Supporting Information, Figure S32).

Thus, when the α-pyrone ring opens, the oxygen atom O2 loses its electron-donating properties as an «ether-oxygen» and becomes an electron-withdrawing group as a «keto-oxygen», which leads to an increase in the positive charge on the carbon atoms C6, C8, and C9′ (See Supporting Information, Figure S32) through the conjugation of the CO group with the benzene ring (Scheme 1A). Therefore, introducing EWG in any of these positions should increase the TS barrier (Scheme 1A). Moreover, introducing a pi-accepting EWG should lead to a stronger TS destabilization than a sigma-acceptor does since the case when two pi-acceptors are in direct conjugation is energetically more unfavourable (Scheme 1B).

Considering that the **IC9O** derivative bearing a COOMe EWG at the C6 position is synthetically accessible from dimethyl iodoterephthalate, we built a computational model for **IC9O-COOMe** and performed the same calculations as for **IC9O** (Figure 3A, B). The obtained data revealed a notable increase (~ 5 kcal/mol) in the value of the TS barrier on the S1 surface. Moreover, the TS point becomes higher than the calculated Frank-Condon point (Figure 3A), along with the significant stabilization (3.5 kcal/mol) of the S1 min point. Consequently, the S1 state of **IC9O-COOMe** should be stable, and the system would need additional thermal energy to overcome the barrier and achieve a conical intersection. Therefore, **IC9O-COOMe** should exhibit fluorescence.

We also noticed that the electron density at the C4 carbon atom of **IC9O** does not change on the path from the FC point to the CI point (See Supporting Information, Figure S32). This fact suggested that there is not a significant relationship between the fluorescent properties of isocoumarins and the nature of the substituents at the C4 position. Therefore, we did not perform preliminary calculations for 1,2,3-triazoles derived from **IC9O** and **IC9O-COOMe**, and turned directly to the synthesis and experimental study of **IC9O-COOMe** and its triazoles as SPAAC products.

The target cyclononyne **IC9O-COOMe** was synthesized from dimethyl iodoterephthalate **1** using the synthetic strategy reported earlier for **IC9O** (Scheme 2).[40] The ester functionality was compatible with the reaction conditions at each step. The synthetic route proceeds via the Sonogashira coupling[47,48] of diester **1**, followed by the electrophile-promoted cyclization[49,50] of alkyne **2**, and then the second Sonogashira reaction with the formation of key isocoumarin intermediate **4**. Conversion of alkyne **4** into the $Co_2(CO)_6$-complex **5** and the subsequent Nicholas reaction[51–58] gave cyclic Co-complex **6**. The latter was successfully subjected to decomplexation from the cobalt fragment, promoted by tetrabutylammonium fluoride (TBAF), which gave the desired target cyclononyne **IC9O-COOMe** (for X-ray see Supporting Information, Figure S23) (Scheme 2).

All reactions proceeded in good to high yields, which allowed cyclononyne **IC9O-COOMe** to be obtained in six synthetic steps with an overall yield of 15%.

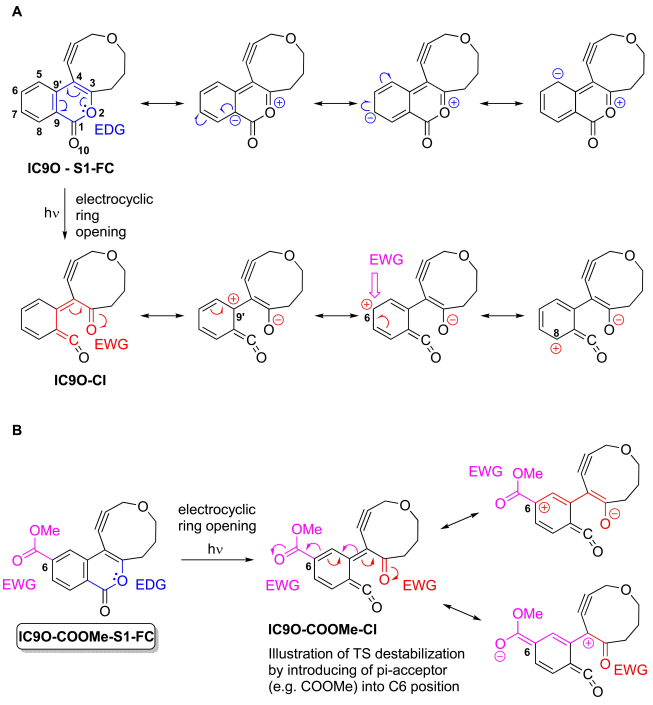

Scheme 1. Changing the electronic effect of O2 atom after an isocoumarin ring-opening as a guide for the design of fluorescent cyclononyne **IC9O-COOMe** (A) and an effect on S1 TS destabilization by pi-acceptors (B).

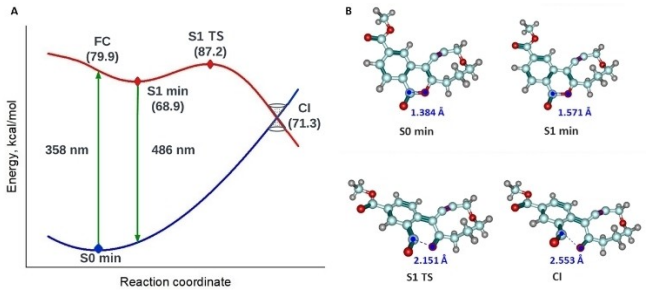

Figure 3. Calculated critical points on the S0 (nevpt2(14,13)/cc-pVDZ:OPLS//PBE0/cc-pVDZ:OPLS) and S1 (nevpt2(14,13)/cc-pVDZ:OPLS//MCPDFT(12,12)-tPBE/cc-pVDZ:OPLS) potential energy surfaces of **IC9O-COOMe** (A) and corresponding **IC9O-COOMe** geometries at critical points (B). The energies (in kcal/mol) shown in the figure are adiabatic energy differences with respect to the S0 min. Calculated maxima for absorption and fluorescence bands (in nm) correspond to vertical transitions between S0 and S1 potential energy surfaces.

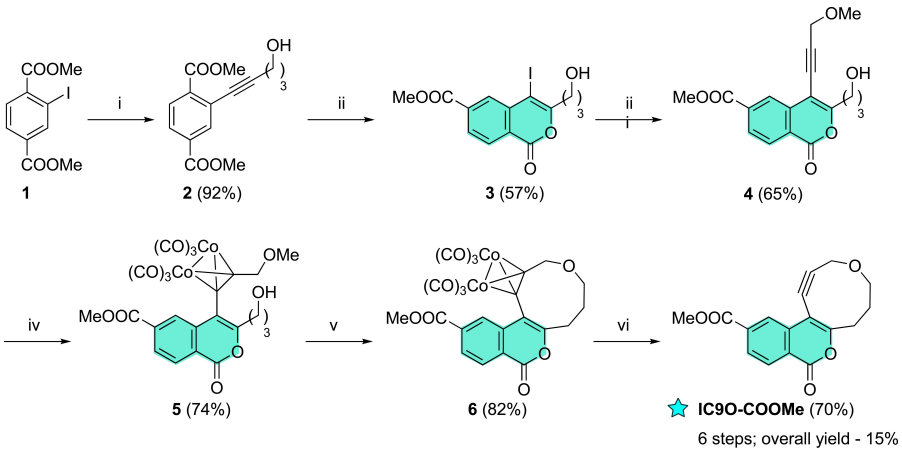

Reagents and conditions: (i) pent-4-yn-1-ol (1.2 equiv), $Pd(PPh_3)_4$ (1 mol%), CuI (4 mol %), NEt_3, THF, 55 °C, 3 h; (ii) I_2 (1 equiv), DCM, 40 °C, 2 h; (iii) methyl propargyl ether (1.5 equiv), $Pd(PPh_3)_4$ (5 mol%), CuI (10 mol %), DIPA (4 equiv), DMF, 55 °C, 3 h; (iv) $Co_2(CO)_8$ (1.2 equiv), benzene, r.t., 2 h; (v) $BF_3{\cdot}Et_2O$ (1.3 equiv), DCM, 0 °C to r.t., 2 h; (vi) TBAF (11 equiv), acetone / H_2O (15:1), 4 h, r.t.

Scheme 2. Synthesis of cyclononyne **IC9O-COOMe**.

It should be emphasized that all isocoumarin derivatives in the synthetic sequence, regardless of the nature of the substituent at the C4 position of the isocoumarin ring, exhibited visible bright blue fluorescence upon excitation with light $\lambda_{ex}=$ 365 nm, which indicated the correctness of the proposed rational design.

An aqueous solution of **IC9O-COOMe** demonstrated blue fluorescence with λ_{max} 481 nm upon excitation at 364 nm (Figure 4) with an absolute quantum yield (Φ_f) of 0.043. We were pleased to note that the calculated absorption and fluorescence band maxima agree with obtained experimental values (compare Figure 3A and Figure 4A, B). An aqueous solution of **IC9O** showed too weak fluorescence to estimate absolute Φ_f (Figure 4B). Therefore, **IC9O**, compared to **IC9O-COOMe**, is referred to here as a non-fluorescent compound.

Comparing the absorption spectra of non-fluorescent **IC9O** and fluorescent **IC9O-COOMe**, a bathochromic shift (28 nm) of the absorption band responsible for the S0→S1 transition is observed. The red-shift of this absorption band correlates well with the decrease of FC point by ~5.5 kcal/mol for **IC9O-COOMe** compared to **IC9O**. We suggest that the bathochromic shift/FC point stabilization is due to the increased aromaticity of the α-pyrone ring in **IC9O-COOMe** compared to **IC9O** because of weaker conjugation of the CO group of the endocyclic ester group with the benzene ring and stronger conjugation of the CO group within the endocyclic oxygen and the whole α-pyrone moiety (Scheme 3). Therefore, it can be assumed that reducing the energy of the FC point by introducing a pi-EWG to the C6 position is another important way to avoid the deactivation of S1 through the opening of the α-pyrone ring.

Next, we turned to studying the reactivity of the cyclononyne **IC9O-COOMe** in SPAAC and investigating the photophysical properties of the corresponding triazoles. Two azides were chosen: a common model benzyl azide and 5-azidomethyl-2′-deoxyuridine (AmdU),[59] a nucleoside-bearing azide used for DNA metabolic labelling (Scheme 4).

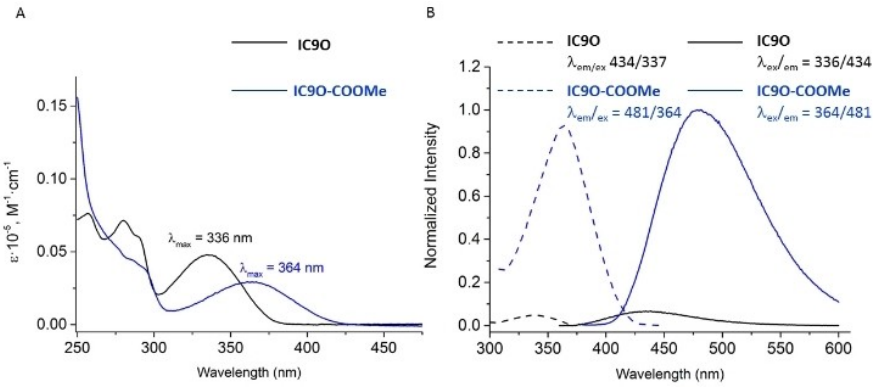

Figure 4. Measured absorption spectra of solutions of **IC9O** and **IC9O-COOMe** in water with 1 v/v% of DMSO ($c=10^{-5}$ M) (A); normalized measured emission (solid line) and excitation (dashed line) spectra of solutions of **IC9O** and **IC9O-COOMe** in water with 1 v/v% of DMSO ($c=10^{-5}$ M) (B).

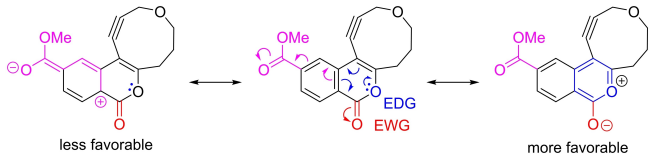

Scheme 3. Resonance structures as the illustration of a red shift in absorption spectra for cycloalkynes with a pi-acceptor at the C6 position.

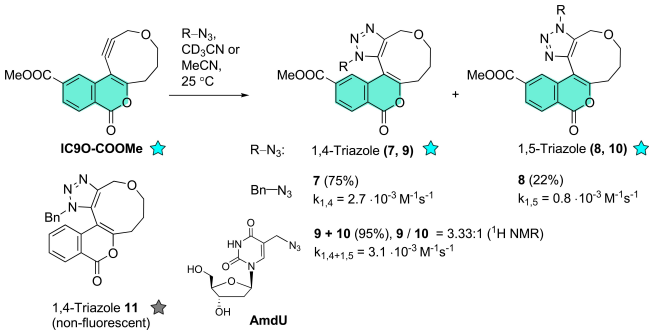

Scheme 4. SPAAC Study for **IC9O-COOMe** and the structure of non-fluorescent triazole **11** synthesized from **IC9O**.

Cyclononyne **IC9O-COOMe** reacted with both azides at 25 °C, giving the corresponding triazoles in excellent yields. Both reactions proceeded regioselectively, forming 1,4-triazoles as the main products, similar to **IC9O**.[40] For the molecular structure of **7** obtained by X-ray (Figure S24) and structural investigation of triazoles **9** and **10** by NMR (Section 2.3.1) and HPLC MS (Section 2.3.2), see Supporting Information.

The second order rate constants for SPAAC between **IC9O-COOMe** and both azides ($k_{BnN3(1,4+1,5)} = 3.5 \times 10^{-3}\ M^{-1}s^{-1}$ and $k_{AmdU(1,4+1,5)} = 3.1 \times 10^{-3}\ M^{-1}s^{-1}$) revealed that SPAAC reactivity of **IC9O-COOMe** does not significantly depend on the azide nature (See Supporting Information, Section 3). We also proved that reactivity could be predicted by DFT calculations[40] using model MeN_3 and a highly bent staggered conformation of **IC9O-COOMe**. For more details, see Supporting Information, Section 6.

Next we turned to investigate the photophysical properties of the obtained triazoles. In the case of benzyl azide, it was possible to isolate the main product 1,4-triazole **7**, the spectra of which were studied. In the case of AmdU, a mixture of 1,4- and 1,5-triazoles was investigated.

As predicted, in the case of **IC9O-COOMe**, the triazole ring formed upon SPAAC did not significantly influence the fluorescent properties of the designed COOMe-substituted isocoumarin system. To our delight, aqueous solutions of Bn- and nucleoside-substituted triazoles were fluorescent in contrast to weakly fluorescent (termed here as non-fluorescent) known *N*-benzyl triazole **11** (Scheme 4) obtained from **IC9O**[40] (Figure 5). Moreover, the triazoles synthesized from **IC9O-COOMe** had similar quantum yields regardless of the nature of the substituent on the azide: absolute Φ_f for the main regioisomer **7** and the mixture of both regioisomers **9** and **10** were 0.047 and 0.032, respectively. Thus, in contrast to known examples of fluorescence quenching when switching from fluorescent cycloalkanes to triazoles,[32,60] here a fluorescent cycloalkyne/triazole pair was developed.

To analyse the influence of water as a solvent for the photophysical properties of cycloalkyne **IC9O-COOMe** and triazole **7**, we measured the absorption and emission spectra of both compounds in a range of solvents with different polarity, different viscosity, and different hydrogen-bonding capabilities. We then compared them with the spectra of aqueous solutions of **IC9O-COOMe** and triazole **7** (for excitation spectra see Supporting Information, Figure S19, S20).

The obtained data revealed that both compounds have stronger fluorescence in polar protic solvents (the strongest fluorescence was found for water solutions) (Figure 6, Figure 7), which are able to stabilize S1 min not only through dipole-dipole interactions but also through the formation of H-bonds.

It is important to note that the absorption maximum responsible for the S0→S1 transition does not change significantly in solvents with different polarity, viscosity, and ability to form H-bonds. On the other hand, a red shift of fluorescence in solvents with higher polarity and especially in solvents with a

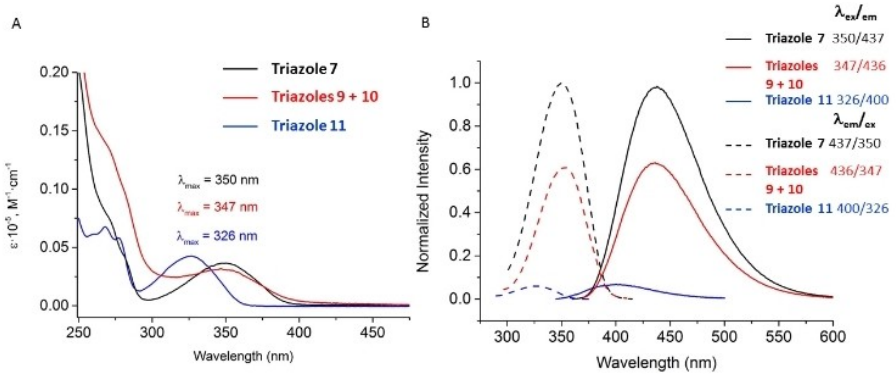

Figure 5. Measured absorption spectra of solutions of triazoles **7**, **9+10**, and **11** in water with 1 v/v% of DMSO ($c = 10^{-5}$ M) (A); normalized measured emission (solid line) and excitation (dashed line) spectra of solutions of triazoles **7**, **9+10** and **11** in water with 1 v/v% of DMSO ($c = 10^{-5}$ M) (B).

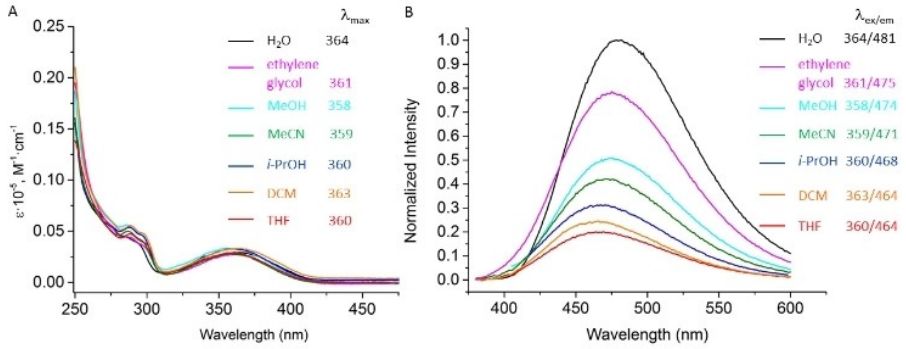

Figure 6. Measured absorption spectra of solutions of cycloalkyne **IC9O-COOMe** in different solvents (see the legend) with 1 v/v% of DMSO ($c = 10^{-5}$ M) (A); normalized measured emission spectra of solutions of cycloalkyne **IC9O-COOMe** in different solvents (see the legend) with 1 v/v% of DMSO ($c = 10^{-5}$ M) (B).

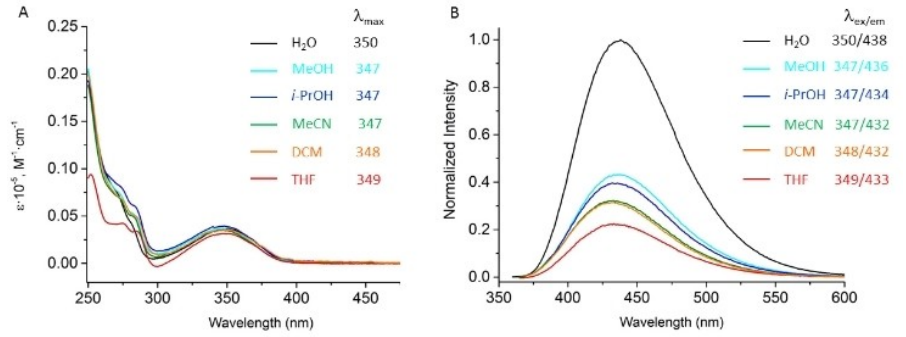

Figure 7. Measured absorption spectra of solutions of triazole **7** in different solvents (see the legend) with 1 v/v% of DMSO ($c = 10^{-5}$ M) (A); normalized measured emission spectra of solutions of triazole **7** in different solvents (see the legend) with 1 v/v% of DMSO ($c = 10^{-5}$ M) (B).

higher ability to form H-bonds illustrates the efficiency of S1 min stabilization through solvation with the contribution of H-bonds in the solvation process. As the strongest fluorescence was found for aqueous solutions of both cycloalkyne and triazole **7**, the developed **IC9O-COOMe**/triazole pair can be viewed as a promising reagent for applications in aqueous media.

The Φ_f and fluorescence lifetime values for the solutions of **IC9O-COOMe** and triazole **7** in various solvents generally correlate well with the observed change in the relative fluorescence intensities: higher values of Φ_f and fluorescence lifetime were estimated for aqueous solutions of the compounds under study (Table 1). These data were used to calculate radiative (k_r) and nonradiative (k_{nr}) S1 decay rates (See Supporting Information, section 4.3).[61,62] We were pleased to note that the calculated k_{nr} for both alkyne **IC9O-COOMe** and triazole **7** were found to be lower in polar protic solvents, with the highest k_r/k_{nr} ratio for water, which proves the ability of polar protic solvents to stabilize S1 min against deactivation pathways. Since the values of Φ_f in solvents other than water were ≤ 0.01, and the fluorescence lifetimes turned out to be at about 1 ns, no quantitative correlation could be built for these solvents.

To prove the developed concept for the rational design of fluorescent cycloalkyne/triazole pairs based on eliminating the deactivation pathway (opening of an isocoumarin ring) by increasing the S1 TS barrier and to show the importance of the nature of the EWG at the C6 position of the isocoumarin ring for fluorescent properties, we turned to the synthesis and theoretical studies of other examples of C6-substituted isocoumarin-fused cycloalkynes/triazoles. Two cycloalkynes – one with a strong pi-acceptor - cyano group (**IC9O-CN**) and another with a strong sigma-acceptor - trifluoromethyl group (**IC9O-CF_3**) were chosen as new target structures (Scheme 5). It should be

Table 1. Photoluminescence quantum yields, lifetimes, radiative and nonradiative decay rates of **IC9O-COOMe** and Triazole **7**.

Solvent[a]	Φ_f	τ_f, ns[b]	k_r 10^9, s^{-1}	k_{nr} 10^9, s^{-1}
IC9O-COOMe				
H_2O	0.043	2.22	0.019	0.4
MeOH	0.005	1.20	0.004	0.8
i-PrOH	0.010	0.95	0.011	1.0
MeCN	0.010	0.64	0.016	1.5
DCM	0.014	1.00	0.014	1.0
THF	0.008	0.58	0.014	1.7
Triazole **7**				
H_2O	0.047	1.95	0.024	0.5
MeOH	0.011	0.94	0.012	1.0
i-PrOH	0.009	0.96	0.009	1.0
MeCN	0.007	0.52	0.013	1.9
DCM	0.005	0.66	0.008	1.5
THF	0.010	0.60	0.017	1.7

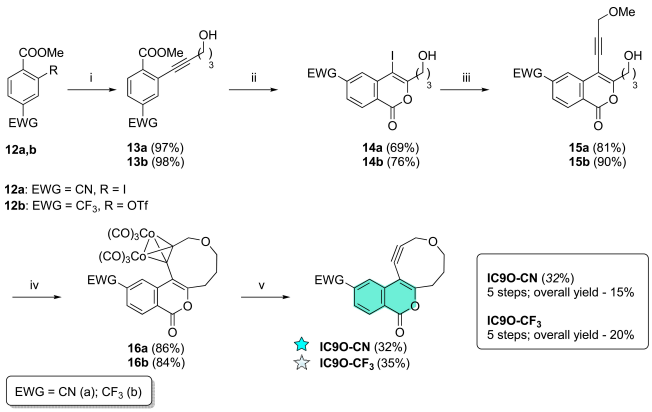

Reagents and conditions: (i) for **12a**: pent-4-yn-1-ol (1.2 equiv), $Pd(PPh_3)_4$ (5 mol%), CuI (10 mol %), NEt_3, 55 °C, 12 h; for **12b**: pent-4-yn-1-ol (2.0 equiv), $PdCl_2(PPh_3)_2$ (5 mol%), CuI (3 mol %), DIPA (5.0 equiv), THF, reflux, 3 h; (ii) I_2 (1.1–1.2 equiv), DCM, 40 °C, 2.5 h; (iii) methyl propargyl ether (2.0 equiv), $Pd(PPh_3)_4$ (5 mol%), CuI (10 mol %), KF (5 equiv), DMF, r.t., 12 h; (iv) Step 1: $Co_2(CO)_8$ (1.5 equiv), DCM (c = 0.01 M), r.t., 2 h; Step 2: $BF_3{\cdot}Et_2O$ (2.0 equiv), DCM (c = 0.002 M), 0 °C to r.t., 0.5 – 2 h; (v) TBAF (5–9 equiv), acetone / H_2O (15:1), 1–2 h, r.t.

Scheme 5. Synthesis of cyclononyne **IC9O-CN** and **IC9O-CF$_3$**.

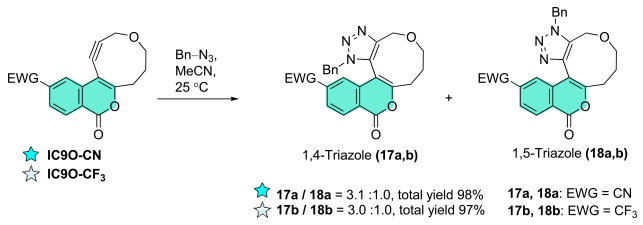

Scheme 6. SPAAC for **IC9O-CN** and **IC9O-CF$_3$**.

emphasized that despite known negative σ*-π hyperconjugation of the CF_3 group, this group can be used as a model of a strong sigma-acceptor compared to real pi-acceptors such as CN and COOMe substituents.[63]

Both cycloalkynes were synthesized using the same synthetic route as for cycloalkyne **IC9O-COOMe**. Syntheses of **IC9O-CN** and **IC9O-CF$_3$** start from the Sonogashira reaction of synthetically available methyl 4-cyano-2-iodobenzoate **12a** and the triflate derivative **12b**, respectively (Scheme 5) (see Supporting Information, Section 2.1).

There are two main differences in the synthetic sequences towards **IC9O-CN** and **IC9O-CF$_3$** compared to the synthetic route for **IC9O-COOMe**. The first one is the use of potassium fluoride as a base for the second Sonogashira coupling (synthesis of alkynes **15a,b**) because DIPA does not work in this case. The second feature is carrying out the complexation of alkynes **15a,b** with cobalt and the subsequent Nicholas cyclization in one pot without isolation of acyclic cobalt complexes. Because of this improvement, despite the fact that the last step – decomplexation from cobalt – gave worse yields for cycloalkynes **IC9O-CN** and **IC9O-CF$_3$** than **IC9O-COOMe**, overall yields for the new structures were comparable to the overall yield for **IC9O-COOMe** (Scheme 5). Both cycloalkynes reacted with benzyl azide providing 1,4- **17a,b** and 1,5-triazoles **18a,b** with the preferable formation of 1,4-isomers **17a,b** (Scheme 6).

The qualitative evaluation ($\lambda_{ex} = 365$ nm) of the fluorescent properties of both cycloalkynes **IC9O-CN** and **IC9O-CF$_3$** and triazoles during the synthesis and purification revealed similar brilliance of fluorescence for the **IC9O-CN** and **IC9O-COOMe** series, while much less intense fluorescence was observed for the **IC9O-CF$_3$** series, which was in line with our expectations regarding the influence of pi- and sigma-acceptors to the destabilization of S1 TS.

Next we turned to the quantitative investigation of the photophysical properties of both new cycloalkyne/triazole pairs. The absorption spectra of alkyne **IC9O-CN** and CN-triazole **17a** resemble the absorption spectra of compounds from the COOMe-series (Figure 8a, Figure 9a).

The absorption maxima of aqueous solutions of **IC9O-CN** and CN-triazole **17a** responsible for the S0→S1 transition were observed at similar wavelengths as for the corresponding **IC9O-COOMe** derivatives and had a red-shift relative to the unsubstituted **IC9O** and triazole **11**. The same absorption maximum for the **IC9O-CF$_3$** series was blue-shifted relative to the compounds with pi-acceptors and red-shifted compared to the unsubstituted **IC9O** series. These changes in absorption spectra support the fundamental role of EWG substituents at the C6 position of the isocoumarin ring for the bathochromic shift and illustrate the greater effect of pi-acceptors compared to sigma-acceptors (see Scheme 3).

There is also a similarity in the emission spectra of aqueous solutions of CN– and COOMe-substituted alkynes and triazoles

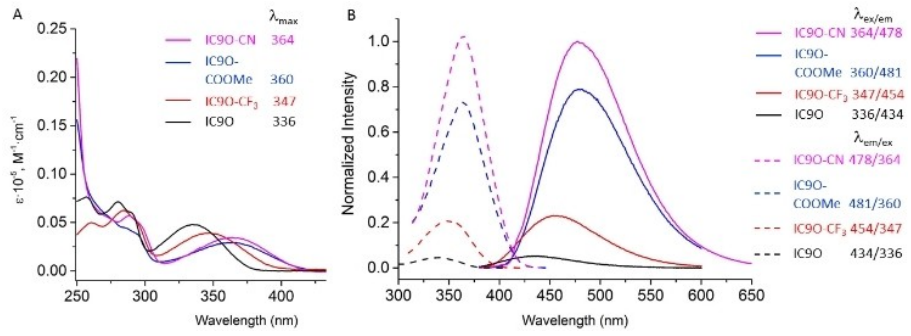

Figure 8. Measured absorption spectra of solutions of all cycloalkynes in water with 1 v/v% of DMSO ($c = 10^{-5}$ M) (A); normalized measured emission (solid line) and excitation (dashed line) spectra of solutions of all cycloalkynes in water with 1 v/v% of DMSO ($c = 10^{-5}$ M) (B).

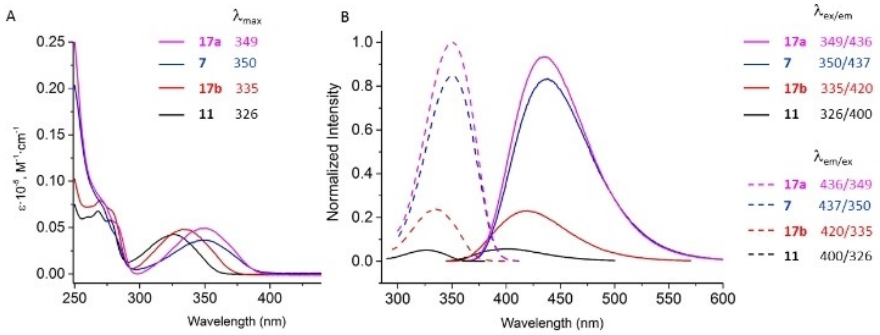

Figure 9. Measured absorption spectra of solutions of triazoles **17a,b** in water with 1 v/v% of DMSO ($c = 10^{-5}$ M) (A); normalized measured emission (solid line) and excitation (dashed line) spectra of solutions of triazoles **17a,b** in water with 1 v/v% of DMSO ($c = 10^{-5}$ M) (B).

(stronger bathochromic shift of the emission maxima as well as an increase in the relative fluorescence intensities) (Figure 8b, Figure 9b). At the same time, CF_3 derivatives lay somewhere between the non-fluorescent **IC9O**/triazole pair and the corresponding derivatives with pi-acceptor groups (Figure 8b, Figure 9b). Regarding other solvents, the same tendency as for the **IC9O-COOMe** series was observed: stronger fluorescence was an attribute of solutions in polar protic solvents. For the absorption, emission and excitation spectra of cycloalkynes in other solvents see Supporting Information, Figures S21, S22.

For both new alkynes **IC9O-CN** and **IC9O-CF_3** and the corresponding 1,4-triazoles **17a,b**, some additional photophysical properties (Φ_f, lifetime values τ, k_r, k_{nr}) were measured (Table 2). Cycloalkyne **IC9O-CN** has very similar photophysical characteristics as its pi-acceptor analog **IC9O-COOMe**. At the same time, cycloalkyne **IC9O-CF_3** still stayed between the non-fluorescent unsubstituted derivative **IC9O** and the fluorescent cycloalkynes with pi-acceptors. Therefore, cycloalkynes with pi-acceptors possess equivalent absolute quantum yields, and similar fluorescence lifetime values, and the values of radiative and nonradiative decays, which illustrates the similar nature of the deactivation of their S1 states and the stabilizing effect if the pi-acceptor groups are at the C6 position (Tables 1, Table 2).

For the cycloalkyne **IC9O-CF_3** and the corresponding triazole **17b**, a significant decrease in Φ_f, fluorescence lifetime, and radiative decay is observed, along with an increase in the rate of nonradiative deactivation of S1 compared to compounds with pi-acceptors.

Finally, we switched back to the calculations to determine the differences in the energies of critical points on the S1 excited state potential energy surface (S1 min, S1 max, and S1/S0 conical intersection) between unsubstituted cycloalkyne **IC9O**, compounds having pi-acceptor groups (**IC9O-COOMe** and **IC9O-CN**) and the cycloalkyne with a sigma-acceptor **IC9O-CF_3**. Therefore, we built two new computational models for **IC9O-CN** and **IC9O-CF_3** and performed the same calculations as described above (see Supporting Information, section 8).

The obtained data for two new cycloalkynes predictably showed the deactivation pathway of S1 by the electrocyclic ring opening of the α-pyrone ring (Figure 10). An important aspect of these additional calculations is the principal role of a pi-acceptor is not only the increase of the S1 TS barrier but also in decreasing the energy of FC and S1 min critical points. All three

Table 2. Photoluminescence quantum yields, lifetimes, radiative and nonradiative decay rates for aqueous solutions of **IC9O-CN and IC9O-CF_3** and triazoles **17a,b**.

Compound	Φ_f	τ_f, ns[b]	k_r 10^9, s^{-1}	k_{nr} 10^9, s^{-1}
IC9O-CN	0.043	2.10	0.020	0.4
IC9O-CF3	0.006	0.64	0.009	1.5
17a	0.035	1.60	0.022	0.6
17b	0.008	0.57	0.014	1.7

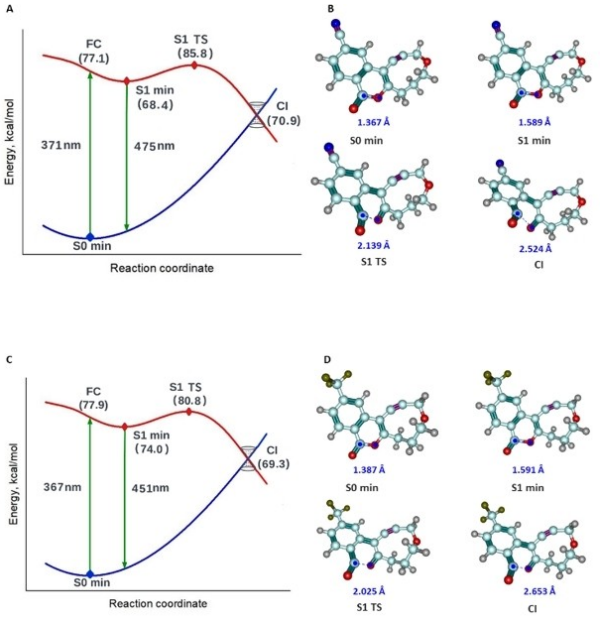

Figure 10. Calculated critical points on the S0 (nevpt2(14,13)/cc-pVDZ:OPLS//PBE0/cc-pVDZ:OPLS) and S1 (nevpt2(14,13)/cc-pVDZ:OPLS//MCPDFT(12,12)-tPBE/cc-pVDZ:OPLS) potential energy surfaces of **IC9O-CN** (A), **IC9O-CF_3** (C), and corresponding **IC9O-CN** (B) and **IC9O-CF_3** (D) geometries at critical points. The energies (in kcal/mol) shown in the figure are adiabatic energy differences with respect to the S0 min. Calculated maxima for absorption and fluorescence bands (in nm) correspond to vertical transitions between S0 and S1 potential energy surfaces.

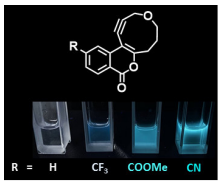

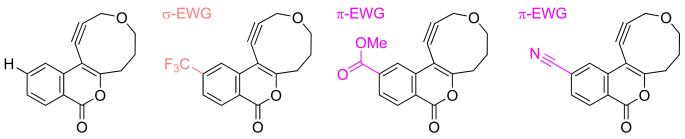

	IC9O	IC9O-CF_3	IC9O-COOMe	IC9O-CN
Calculated data (all in kcal/mol)				
FC	85.6	77.9	79.9	77.1
S1 min	72.3	74.0	68.9	68.4
S1 TS	82.3	80.8	87.2	85.8
CI	67.2	69.3	71.3	70.9
Δ(S1 TS-FC)	−3.3	2.9	7.3	8.7
Δ(S1 TS-S1 min)	10.3	6.8	18.3	17.7
Experimental data (in H_2O)				
Φ_f	n.d.	0.0006	0.043	0.043
τ, ns	n.d.	0.64	2.22	2.10
$k_r \cdot 10^9$, s^{-1}	n.d.	0.009	0.019	0.020
$k_{nr} \cdot 10^9$, s^{-1}	n.d.	1.5	0.4	0.4
λ_{ex}, nm	336	347	364	364
λ_{em}, nm	434	454	481	477

Figure 11. Summary of calculated and measured characteristics for the series of isocoumarin-fused cycloalkynes (in the upper left corner, there is a photo of solutions of cycloalkynes in MeOH with 10 v/v% of DMSO ($c = 5 \cdot 10^{-4}$ M) under irradiation ($\lambda = 365$ nm)).

stabilizing actions are very important for preventing the deactivation of the S1 state through the opening of the α-pyrone ring.

A summary of the measured characteristics and calculated energetic parameters for the entire series of cycloalkynes is illustrated in Figure 11. There is a direct trend towards an increase in k_r and a decrease in k_{nr} upon passing from sigma-EWG to pi-EWG substituted compounds, which is in good agreement with the calculated increase in the S1 TS barrier. Both pi-acceptor groups lead to higher S1 TS barriers and also stabilize FC and S1 min points. The sigma-acceptor imparts weak fluorescent properties to **IC9O-CF_3** compared to **IC9O** only by lowering the energy of the FC point relative to TS S1, despite the fact that in the case of **IC9O-CF3** the difference in S1 min and S1 TS point becomes smaller compared to **IC9O**.

Conclusions

In summary, based on a rational modification of non-fluorescent isocoumarin-fused cyclononyne **IC9O**, we developed fluorescent oxacyclononynes **IC9O-EWG**, which provide fluorescent triazoles upon SPAAC.

Employing multi-configurational ab initio and DFT methodologies, we demonstrated that the deactivation of the S1 excited state of non-fluorescent isocoumarin-fused cyclononyne **IC9O** occurs through electrocyclic ring-opening by cleavage of the ester bond of the α-pyrone cycle. Based on the electron-density distribution for the structure that corresponds to the barrier on the path on the S1 potential energy surface, we first predicted and then proved, theoretically and experimentally, that introducing an acceptor group at the C6 position of the isocoumarin ring increases the barrier for S1 excited state deactivation and impedes the nonradiative deactivation of the S1 state. Moreover, we have shown that the nature of the acceptor group is critical, and only pi-acceptors lead to a large increase in the S1 min – S1 TS barrier. It was also found that additional stabilization of the S1 states from nonradiative deactivation is associated with a decrease in the energy of the FC point for both sigma- and pi-acceptor groups and stabilization of the S1 min point only for pi-acceptors.

The applicability of our approach was demonstrated by the design of further fluorescent cyclononyne/triazole pairs. Indeed, the synthesized isocoumarin-fused oxacyclononynes with pi-acceptor groups at the C6 position (**IC9O-COOMe** and **IC9O-CN**) along with the corresponding triazoles obtained by SPAAC possessed blue fluorescence regardless of the azide nature. The search for applications of the developed fluorescent **IC9O-EWG**/triazole pairs is ongoing.

Experimental Section

Hexacarbonyl (methyl 3-(3-hydroxypropyl)-4-(3-methoxyprop-(1,2-η²)-1-yn-1-yl)-1-oxo-1*H*-isochromene-6-carboxylate)dicobalt (5): To a solution of an alkynylisocoumarin **4** (400 mg, 1.21 mmol, 1.00 equiv.) in benzene (121 mL) was added octacarbonyldicobalt (496 mg, 1.45 mmol, 1.20 equiv.), and the mixture was stirred under a flow of Ar at room temperature for 2 h (TLC control). After completion of the reaction, the solvent was evaporated under reduced pressure, and the residue was purified by column chromatography on silica gel (eluent: hexane/EtOAc = 2:1) that gave Co-complex **5** (550 mg, 74%) as a dark-brown oil. ^{1}H NMR (400 MHz, Acetone-d_6) δ 8.80 (s, 1H), 8.37 (d, J = 7.5 Hz, 1H), 8.17 (d, J = 7.5 Hz, 1H), 5.02 (s, 2H), 3.96 (s, 3H), 3.77 (br s, m, 3H – CH_2, OH), 3.59 (s, 3H), 3.10 (br s, 2H), 2.09 (s, 2H). ^{13}C NMR (101 MHz, Acetone-d_6) δ 200.4, 166.4, 160.8, 160.5, 138.5, 135.9, 130.7, 128.8, 126.3, 124.2, 110.5, 99.5, 79.3, 75.0, 61.7, 59.0, 52.8, 35.4 (overlaps with the

solvent signal, appears in DEPT), 34.3 (overlaps with the solvent signal, appears in DEPT). HRMS ESI m/z: $[M+Na]^+$ Calcd for $C_{24}H_{18}Co_2O_{12}Na^+$: 638.9354; Found: 638.9362, $[M\text{-}1CO+Na]^+$ Calcd for $C_{23}H_{18}Co_2O_{11}Na^+$: 610.9405; Found: 610.9411, $[M\text{-}2CO+Na]^+$ Calcd for $C_{22}H_{18}Co_2O_{10}Na^+$: 582.9456; Found: 582.9463.

Additional information on the chemical synthesis and the analysis of the target compound is available via the Chemotion repository: https://dx.doi.org/10.14272/reaction/SA-FUHFF-UHFFFADPSC-NAVZHPYOUB-UHFFFADPSC-NUHFF-NUHFF-NUHFF-ZZZ.2.

Hexacarbonyl (methyl (1,2-η²)-1,2-didehydro-9-oxo-5,6,7,9-tetrahydro-3*H*-oxonino[5,6-*c*]isochromene-12-carboxylate)dicobalt (6): A stirred solution of acyclic Co-complex **5** (365 mg, 0.592 mmol, 1.00 equiv.) in dry DCM (c = 0.0025 M, 240 mL) was cooled to 0 °C under an argon atmosphere. Then boron trifluoride diethyl etherate complex (109 mg, 94.8 μL, 0.770 mmol, 1.30 equiv.) was added in one portion. A cooling bath was immediately removed, and the resulting solution was allowed to warm to room temperature and then stirred at this temperature for 2 h (TLC control). Then the reaction mixture was quenched with a 5% aqueous solution of $NaHCO_3$ (200 mL). The organic layer was separated, washed with brine (200 mL), dried over anhydrous Na_2SO_4, and concentrated under reduced pressure to yield a crude product, which was purified by column chromatography on silica gel (eluent: hexane/EtOAc = 3:1) that gave cyclic Co-complex **6** (284 mg, 82%) as a dark-brown oil. ^{1}H NMR (400 MHz, Acetone-d_6) δ 9.11 (s, 1H), 8.43–8.35 (br m, 1H), 8.24–8.15 (br m, 1H), 5.31 (br s, 2H), 3.93 (br s, 3H), 3.68 (br s, 2H), 3.01 (br s, 2H), 2.25 (br s, 2H). ^{13}C NMR (101 MHz Acetone-d_6) δ 200.5, 166.3, 161.1, 158.5, 138.5, 136.1, 130.7, 128.9, 125.3, 124.6, 111.4, 95.5, 82.5, 70.8, 64.2, 52.8, 33.9, 28.8. HRMS (ESI) m/z: $[M+Na]^+$ Calcd for $C_{23}H_{14}Co_2O_{11}Na^+$: 606.9092; Found: 606.9100.

Additional information on the chemical synthesis and the analysis of the target compound is available via the Chemotion repository: https://dx.doi.org/10.14272/reaction/SA-FUHFF-UHFFFADPSC-YSY-KOEVOUK-UHFFFADPSC-NUHFF-NUHFF-NUHFF-ZZZ.1.

General procedure for the synthesis of Co-complex and the Nicholas cyclization under one-pot conditions: In a flame-dried three-necked round bottom flask under an argon atmosphere, an alkyne (1.00 equiv.) was dissolved in anhydrous DCM (c = 0.01 M), and octacarbonyldicobalt (1.50 equiv.) was added. The mixture was stirred under a flow of argon at room temperature for the corresponding time (TLC control). After completion of the reaction, the reaction mixture was diluted with DCM (c = 0.002 M) and cooled to 0 °C, then boron trifluoride diethyl etherate complex (2.00 equiv.) was added in one portion. A cooling bath was immediately removed, and the resulting solution was allowed to warm to room temperature and then stirred at this temperature until the completion of the reaction (TLC). Then the reaction mixture was quenched with a 5% aqueous solution of $NaHCO_3$. The organic layer was separated, washed with brine, dried over anhydrous Na_2SO_4, and concentrated under reduced pressure to yield a crude product, which was purified by column chromatography.

Hexacarbonyl ((1,2-η²)-1,2-didehydro-9-oxo-5,6,7,9-tetrahydro-3*H*-oxonino[5,6-c]isochromene-12-carbonitrile)dicobalt (16a): Co-complex **16a** was synthesized in accordance with the general procedure for the one-pot Co-complexation/Nicholas reaction from alkyne **15a** (200 mg, 0.673 mmol, 1.00 equiv.), $Co_2(CO)_8$ (345.0 mg, 1.01 mmol, 1.50 equiv.), in DCM (c = 0.01, 67.0 mL) at room temperature for 2 h (TLC control: hexane/ethyl acetate 2:1). Nicholas cyclization was performed after dilution of the reaction mixture with DCM (c = 0.002 M, added amount of DCM is 270 mL) by adding of boron trifluoride diethyl etherate complex (190.8 mg, 1.34 mmol, 2 equiv.). The reaction time was 30 min. Purification of the crude product by column chromatography (eluent: hexane/ethyl acetate = 7:1) gave cyclic Co-complex **16a** (320 mg, 86%) as a dark-brown powder. M. p. = 61–62 °C. ^{1}H NMR (400 MHz, Acetone-d_6) δ 8.81 (s, 1H), 8.43 (d, J = 8.2 Hz, 1H), 8.01 (d, J = 8.2 Hz, 1H), 5.33 (br s, 2H), 3.71 (br s, 2H), 3.02 (br s, 2H), 2.26 (br s, 2H). ^{13}C NMR (126 MHz, Acetone-d_6) δ 200.2, 160.6, 159.4, 138.8, 131.4, 131.2, 127.9, 124.5, 118.1, 117.9, 110.8, 95.9, 81.6, 70.8, 64.3, 33.9, 28.7. HRMS (ESI) m/z: $[M\text{-}2CO+Na]^+$ Calcd for $C_{20}H_{11}Co_2NO_7Na^+$: 517.9092; Found: 517.9104.

Additional information on the chemical synthesis and the analysis of the target compound is available via the Chemotion repository: https://dx.doi.org/10.14272/reaction/SA-FUHFF-UHFFFADPSC-ITVN-FIWCBF-UHFFFADPSC-NUHFF-NUHFF-NUHFF-ZZZ.

Hexacarbonyl ((1,2-η²)-1,2-didehydro-12-(trifluoromethyl)-3,5,6,7-tetrahydro-9*H*-oxonino[5,6-c]isochromen-9-one)dicobalt (16b): Co-complex **16b** was synthesized in accordance with the general procedure for the one-pot Co-complexation/Nicholas reaction from alkyne **15b** (160 mg, 0.470 mmol, 1.00 equiv.), $Co_2(CO)_8$ (241 mg, 0.705 mmol, 1.50 equiv.), in DCM (c = 0.01 M, 47.0 mL) at room temperature for 2 h (TLC control: hexane/ethyl acetate 1:1). Nicholas cyclization was performed after dilution of the reaction mixture with DCM (c = 0.002 M, the added amount of DCM is 200 mL) by adding of boron trifluoride diethyl etherate complex (133.2 mg, 0.938 mmol, 2 equiv.). The reaction time was 30 min. Purification of the crude product by column chromatography (eluent: hexane/ethyl acetate = 5:1) gave cyclic Co-complex **16b** (235 mg, 84%) as a dark-brown powder. M. p. = 67–68 °C. ^{1}H NMR (500 MHz, Acetone-d_6) δ 8.80 (br s, 1H), 8.47 (br s, 1H), 7.97 (br s, 1H), 5.32 (br s, 2H), 3.70 (br s, 2H), 3.02 (s, 2H), 2.26 (br s, 2H). ^{13}C NMR (126 MHz, Acetone-d_6) δ 200.2, 160.7, 159.2, 139.0, 135.7 (q, J = 32.7 Hz), 131.6, 125.0 (q, J = 3.4 Hz), 124.7 (q, J = 272.6 Hz), 124.5, 121.2 (q, J = 3.4 Hz), 111.1, 95.7, 81.9, 70.8, 64.2, 33.9, 28.8. HRMS (ESI) m/z: $[M\text{–}CO+Na]^+$ Calcd for $C_{21}H_{11}Co_2F_3O_8Na^+$: 588.8962; Found: 588.8976; m/z: $[M\text{-}2CO+Na]^+$ Calcd for $C_{20}H_{11}Co_2F_3O_7Na^+$: 560.9013; Found: 560.9010.

Additional information on the chemical synthesis and the analysis of the target compound is available via the Chemotion repository: https://dx.doi.org/10.14272/reaction/SA-FUHFF-UHFFFADPSC-UMFI-QYMKBO-UHFFFADPSC-NUHFF-NUHFF-NUHFF-ZZZ.

General procedure for decomplexation of cyclic Co-complexes using TBAF: To a stirred solution of cyclic Co complex (1.00 equiv.) in a mixture of acetone/water (15:1, v/v, c = 0.006 M), tetrabutylammonium fluoride hydrate or trihydrate (TBAF hydrate or TBAF trihydrate) (5–11 equiv.) was added in several portions with the interval of 40 min (TLC control). After completion of the reaction, the reaction mixture was filtered through a thin pad of Celite, the sorbent was washed with acetone, and the resulting solution was concentrated under reduced pressure at 28 °C up to ~1/5 of the original volume; the resulting mixture was mixed with ethyl acetate and brine. The organic layer was separated, and the aqueous layer was extracted with ethyl acetate. The combined organic layers were washed three times with brine, dried over anhydrous Na_2SO_4, and the solvent was evaporated under reduced pressure at 28 °C. The crude product was purified by column chromatography on silica gel.

Methyl 1,2-didehydro-9-oxo-5,6,7,9,–tetrahydro-3*H*-oxocino[5,6-*c*]isochromene-12-carboxylate (IC9O-COOMe): **IC9O-COOMe** was synthesized in accordance with the general procedure for Co-decomplexation from cyclic Co-complex **6** (200 mg, 0.342 mmol, 1.00 equiv.), TBAF hydrate (984 mg, 3.77 mmol, 11.0 equiv., was added in 5 portions), in the mixture of acetone/H_2O (15:1, v/v) (c = 0.006, 57.0 mL) at room temperature. The reaction time was 4 h.

Purification of the crude product by column chromatography (eluent: benzene/ethyl acetate = 30 : 1) gave **IC9O-COOMe** (71.0 mg, 70%) as a light yellow powder. **IC9O-COOMe** starts to decompose at 136 °C without melting. ^{1}H NMR (400 MHz, Acetone-d_6) δ 8.30 (d, J = 8.2 Hz, 1H), 8.16 (d, J = 1.3 Hz, 1H), 8.13 (dd, J = 8.2, 1.3 Hz, 1H), 4.48 (s, 2H), 3.98 (s, 3H), 3.8 (t, J = 5.6 Hz, 2H), 2.94–2.91 (t, J = 6.0 Hz, 2H), 2.16–2.10 (m, 2H). ^{13}C NMR (101 MHz, Acetonitrile-d_3) δ 167.6, 166.5, 161.6, 137.2, 136.0, 130.8, 129.2, 125.8, 123.5, 105.3, 101.3, 89.6, 69.8, 61.0, 53.4, 31.0, 29.7. HRMS (ESI) m/z: $[M+Na]^+$ Calcd for $C_{17}H_{14}O_5Na^+$: 321.0733; Found: 321.0738.

Additional information on the chemical synthesis and the analysis of the target compound is available via the Chemotion repository: https://dx.doi.org/10.14272/reaction/SA-FUHFF-UHFFFADPSC-MTTHMHHBSG-UHFFFADPSC-NUHFF-NUHFF-NUHFF-ZZZ.

1,2-Didehydro-9-oxo-5,6,7,9-tetrahydro-3*H*-oxonino[5,6-*c*]-isochromen-12-carbonitrile (IC9O-CN): **IC9O-CN** was synthesized in accordance with the general procedure for Co-decomplexation from cyclic Co-complex **16a** (197 mg, 0.357 mmol, 1.00 equiv.), TBAF trihydrate (564 mg, 1.79 mmol, 5.00 equiv. was added in 1 portion), in the mixture of acetone/H_2O (15 : 1, v/v) (c = 0.006 M, 60.0 mL). The reaction time was 1 h. Purification of the crude product by column chromatography (eluent: hexane/ethyl acetate = 5 : 1) gave **IC9O-CN** (30.0 mg, 32%) as a slightly yellow powder. **IC9O-CN** starts to decompose at 149 °C without melting. ^{1}H NMR (500 MHz, Acetonitrile-d_3) δ 8.28 (d, J = 8.2 Hz, 1H), 7.91 (s, 1H), 7.81 (dd, J = 8.2, 1.5 Hz, 1H), 4.43 (s, 2H), 3.86 (t, J = 5.6, 2H), 2.90 (t, J = 6.0, 2H), 2.10 - 2.05 (m, 2H). ^{13}C NMR (126 MHz, Acetonitrile-d_3) δ 168.5, 161.1, 136.2, 131.8, 131.2, 129.2, 123.4, 119.3, 105.6, 101.2, 88.90, 69.8, 60.9, 31.0, 29.6. One signal is missing due to overlapping with the solvent signal. HRMS (ESI) m/z: $[M+Na]^+$ Calcd for $C_{16}H_{11}NO_3Na^+$: 266.0812; Found: 266.0801.

Additional information on the chemical synthesis and the analysis of the target compound is available via the Chemotion repository: https://dx.doi.org/10.14272/reaction/SA-FUHFF-UHFFFADPSC-FUHXXZUHXV-UHFFFADPSC-NUHFF-NUHFF-NUHFF-ZZZ.

1,2-Didehydro-12-(trifluoromethyl)-9-oxo-3,5,6,7-tetrahydro-9*H*-oxonino[5,6-*c*]isochromen-9-one (IC9O-CF$_3$): **IC9O-CF$_3$** was synthesized in accordance with the general procedure for Co-decomplexation from cyclic Co-complex **16b** (120 mg, 0.202 mmol, 1.00 equiv.), TBAF trihydrate (510 mg, 1.62 mmol, 9 equiv., was added in 2 portions) in the mixture of acetone/H_2O (15 : 1, v/v) (c = 0.006 M, 34.0 mL) at room temperature. Reaction time was 2 h (TLC control). Purification of the crude product by column chromatography (eluent: hexane/ethyl acetate = 5 : 1) gave **IC9O-CF$_3$** (22 mg, 35%) as a white powder. **IC9O-CF$_3$** starts to decompose at 142 °C without melting. ^{1}H NMR (400 MHz, Acetonitrile-d_3) δ 8.34 (d, J = 8.2 Hz, 1H), 7.84 - 7.76 (m, 2H), 4.43 (s, 2H), 3.84 (t, J = 5.6, 2H), 2.93–2.89 (m, 2H), 2.11–2.05 (m, 2H, overlapping with solvent signal). ^{13}C NMR (101 MHz, Acetonitrile-d_3) δ 168.3, 161.2, 136.7 (q, J = 32.8 Hz), 136.5, 131.6, 125.4 (q, J = 3.6 Hz), 124.5 (q, J = 272.4 Hz), 123.4, 121.9 (q, J = 4.1 Hz), 105.6, 101.7, 89.1, 69.9, 60.9, 31.1, 29.7. HRMS (ESI) m/z: $[M+Na]^+$ Calcd for $C_{16}H_{11}F_3O_3Na^+$: 331.0552; Found: 331.0560.

Additional information on the chemical synthesis and the analysis of the target compound is available via the Chemotion repository: https://dx.doi.org/10.14272/reaction/SA-FUHFF-UHFFFADPSC-QTFCYZQONW-UHFFFADPSC-NUHFF-NUHFF-NUHFF-ZZZ.

General procedure for SPAAC with benzyl azide: To a stirred solution of cycloalkyne **IC9O-EWG** (1.00 equiv.) in acetonitrile (c = 0.01 M), benzyl azide (2.00 equiv.) was added in one portion. The resulting solution was stirred at room temperature for 12 h. The solvent was removed under reduced pressure, and the crude product was purified by column chromatography on silica gel to give isomeric 1,4-triazole and 1,5-triazole.

SPAAC of IC9O-COOMe with BnN3: 1,4-Triazole **7** and 1,5-triazole **8** were synthesized in accordance with the general procedure for SPAAC from **IC9O-COOMe** (15.0 mg, 0.053 mmol, 1.00 equiv.) in acetonitrile (5.30 mL), benzyl azide (14.0 mg 0.105 mmol, 2.00 equiv.). Purification of the crude products by column chromatography (eluent: benzene/ethyl acetate = 3 : 1) gave isomeric 1,4-triazole **7** (16.2 mg, 75%) as a white powder and 1,5-triazole **8** (4.7 mg, 22%) a white powder.

Methyl 1-benzyl-10-oxo-1,4,6,7,8,10-hexahydroisochromeno-[4′,3′ : 5,6]oxonino[3,4-*d*][1,2,3]triazole-13-carboxylate (**7**): Mp 188–190 °C. ^{1}H NMR (400 MHz, Acetone-d_6) δ 8.24 (d, J = 8.2 Hz, 1H), 7.98 (dd, J = 8.2, 1.3 Hz, 1H), 7.13–7.08 (m, 3H), 7.07 (d, J = 1.3 Hz, 1H), 7.02–6.97 (m, 2H), 5.51 (d, J = 15.0 Hz, 1H), 5.20 (d, J = 15.0 Hz, 1H), 4.69 (d, J = 14.2 Hz, 1H), 4.33 (d, J = 14.2 Hz, 1H), 3.73 (s, 3H), 3.62–3.58 (m, 2H), 2.12–2.07 (m, 1H), 1.89–1.82 (m, 1H), 1.72–1.62 (m, 1H), 1.58–1.49 (m, 1H). ^{13}C NMR (101 MHz, Acetone-d_6) δ 164.9, 160.4, 159.7, 147.5, 136.3, 135.9, 135.0, 129.9, 128.6, 128.3, 128.2, 128.1, 128.1, 124.3, 122.9, 102.7, 71.7, 66.8, 52.4, 52.0, 29.8, 27.3. HRMS (ESI) m/z: $[M+H]^+$ Calcd for $C_{24}H_{22}N_3O_5^+$: 432.1554; Found: 432.1555.

Additional information on the chemical synthesis and the analysis of the target compound is available via the Chemotion repository: https://dx.doi.org/10.14272/reaction/SA-FUHFF-UHFFFADPSC-WIUKQDBNTS-UHFFFADPSC-NUHFF-NUHFF-NUHFF-ZZZ.

Methyl 3-benzyl-10-oxo-3,4,6,7,8,10-hexahydroisochromeno-[4′,3′ : 5,6]oxonino[3,4-*d*][1,2,3]triazole-13-carboxylate (**8**): Mp 210–212 °C.^{1}H NMR (400 MHz, Acetonitrile-d_3) δ 8.33 (d, J = 8.2 Hz, 1H), 8.07 (d, J = 8.2 Hz, 1H), 7.72 (s, 1H), 7.43–7.37 (m, 3H), 7.30 (d, J = 7.4 Hz, 2H), 5.69–5.67 (two doublets of AB system with very close chemical shifts, 2H), 4.84 (d, J = 15.0 Hz, 1H), 4.27 (d, J = 15.0 Hz, 1H), 3.87 (s, 3H), 3.71–3.64 (br m, 2H), 2.59–2.55 (br m, 1H), 2.40–2.33 (br m, 1H), 1.77 (br s, 1H), 1.72–1.63 (br m, 1H). HRMS (ESI) m/z: $[M+H]^+$ Calcd for C24H22 N3O5$^+$:432.1554; Found: 432.1557.

Additional information on the chemical synthesis and the analysis of the target compound is available via the Chemotion repository: https://dx.doi.org/10.14272/reaction/SA-FUHFF-UHFFFADPSC-WIUKQDBNTS-UHFFFADPSC-NUHFF-NUHFF-NUHFF-ZZZ.

SPAAC IC9O-CN with BnN$_3$: 1,4-Triazole **17a** and 1,5-triazole **18a** were synthesized in accordance with the general procedure for SPAAC from **IC9O-CN** (14.0 mg, 0.0528 mmol, 1.00 equiv.) in acetonitrile (5.30 mL) and benzyl azide (14.1 mg 0.106 mmol, 2.00 equiv.). Purification of the crude products by column chromatography (eluent: DCM/acetonitrile = 10 : 1 + 0.5% MeOH) gave isomeric 1,4-triazole **17a** (15.5 mg, 74%) as a white powder and 1,5-triazole **18a** (5.0 mg, 24%) as a white powder.

1-benzyl-10-oxo-1,4,6,7,8,10-hexahydroisochromeno[4′,3′ : 5,6]-oxonino[3,4-*d*][1,2,3]triazole-13-carbonitrile (17a): M. p. = 231–232 °C. ^{1}H NMR (400 MHz, Acetone-d_6) δ 8.38 (d, J = 8.2 Hz, 1H), 7.89 (dd, J = 8.2, 1.4 Hz, 1H), 7.31–7.07 (m, 6H), 5.64 (d, J = 15.1 Hz, 1H), 5.37 (d, J = 15.1 Hz, 1H), 4.76 (d, J = 14.2 Hz, 1H), 4.47 (d, J = 14.2 Hz, 1H), 3.78–3.60 (m, 2H), 2.25–2.16 (m, 1H), 2.00–1.89 (m, 1H), 1.84–1.72 (m, 1H), 1.70–1.59 (m, 1H). ^{13}C NMR (126 MHz, Acetone-d_6) δ 161.6, 160.8, 148.6, 137.6, 135.9, 131.5, 131.2, 129.5, 129.3, 129.2, 128.7, 128.5, 123.5, 119.2, 117.9, 102.9, 72.4, 67.5, 53.3, 30.9, 28.18. HRMS (ESI) m/z: $[M+Na]^+$ Calcd for $C_{23}H_{18}N_4O_3Na^+$:421.1271; Found: 421.1269.

Additional information on the chemical synthesis and the analysis of the target compound is available via the Chemotion repository:

https://dx.doi.org/10.14272/reaction/SA-FUHFF-UHFFFADPSC-AHEUGFYYUD-UHFFFADPSC-NUHFF-NUHFF-NUHFF-ZZZ.

3-benzyl-10-oxo-3,4,6,7,8,10-hexahydroisochromeno[4′,3′:5,6]-oxonino[3,4-*d*][1,2,3]triazole-13-carbonitrile (**18 a**): M. p. = 221–222 °C. ^{1}H NMR (400 MHz, Acetone-d_6) δ 8.38 (dd, J = 8.2, 0.5 Hz, 1H), 7.90 (dd, J = 8.2, 1.5 Hz, 1H), 7.52 (d, J = 1.0 Hz, 1H), 7.45–7.31 (m, 5H), 5.79 (s, 2H), 4.96 (d, J = 14.8 Hz, 1H), 4.46 (d, J = 14.8 Hz, 1H), 3.85–3.65 (m, 2H), 2.58 (br s, 1H), 2.41 (br s, 1H), 1.90 (br s, 1H), 1.75 (br s, 1H). HRMS (ESI) m/z: $[M+Na]^+$ Calcd for $C_{23}H_{18}N_4O_3Na^+$:421.1271; Found: 421.1275.

Additional information on the chemical synthesis and the analysis of the target compound is available via the Chemotion repository: https://dx.doi.org/10.14272/reaction/SA-FUHFF-UHFFFADPSC-AHEUGFYYUD-UHFFFADPSC-NUHFF-NUHFF-NUHFF-ZZZ.

SPAAC IC9O-CF$_3$ with BnN$_3$: 1,4-Triazole **17 b** and 1,5-triazole **18 b** were synthesized in accordance with the general procedure for SPAAC from **IC9O-CF$_3$** (10.0 mg, 0.032 mmol, 1.00 equiv.) in acetonitrile (3.70 mL), benzyl azide (8.6 mg 0.065 mmol, 2.00 equiv.). Purification of the crude products by column chromatography (eluent: DCM/acetonitrile = 10 : 1) gave isomeric 1,4-triazole **17 b** (10.5 mg, 73 %) as a yellow powder and 1,5-triazole **18 b** (3.5 mg, 24 %) as a white powder.

1-benzyl-13-(trifluoromethyl)-4,6,7,8-tetrahydroisochromeno-[4′,3′:5,6]oxonino[3,4-*d*][1,2,3]triazol-10(1*H*)-one (**17 b**): M. p. = 236–237 °C. ^{1}H NMR (500 MHz, Acetone-d_6) δ 8.46 (d, J = 8.3 Hz, 1H), 7.88 (dd, J = 8.3, 1.1 Hz, 1H), 7.29–7.21 (m, 3H), 7.19–7.12 (m, 2H), 6.99 (s, 1H), 5.66 (d, J = 15.0 Hz, 1H), 5.31 (d, J = 15.0 Hz, 1H), 4.77 (d, J = 14.2 Hz, 1H), 4.46 (d, J = 14.2 Hz, 1H), 3.81–3.62 (m, 2H), 2.26–2.13 (m, 1H), 1.97–1.88 (m, 1H), 1.83–1.73 (m, 1H), 1.70–1.60 (m, 1H). ^{13}C NMR (126 MHz, Acetone-d_6) δ 161.5, 160.9, 148.5, 137.8, 136.57 (q, J = 32.7 Hz), 135.9, 131.7, 129.5, 129.2, 129.1, 128.8, 125.4 (q, J = 3.5 Hz), 124.2 (q, J = 272.8 Hz), 123.6 (q, J = 1.4 Hz), 121.2 (q, J = 4.1 Hz), 103.4, 72.5, 67.6, 53.2, 30.8, 28.2. HRMS (ESI) m/z: $[M+Na]^+$ Calcd for $C_{23}H_{18}F_3N_3O_3Na^+$:464.1192; Found: 464.1196.

Additional information on the chemical synthesis and the analysis of the target compound is available via the Chemotion repository: https://dx.doi.org/10.14272/reaction/SA-FUHFF-UHFFFADPSC-WEQVDYVYYA-UHFFFADPSC-NUHFF-NUHFF-NUHFF-ZZZ.

3-benzyl-13-(trifluoromethyl)-4,6,7,8-tetrahydroisochromeno-[4′,3′:5,6]oxonino[3,4-*d*][1,2,3]triazol-10(3*H*)-one (**18 b**): M. p. = 211–212 °C. ^{1}H NMR (400 MHz, Acetone-d_6) δ 8.44 (d, J = 8.3 Hz, 1H), 7.87 (dd, J = 8.3, 1.2 Hz, 1H), 7.49–7.30 (m, 6H), 5.80 (s, 2H), 4.97 (d, J = 15.0 Hz, 1H), 4.45 (d, J = 15.0 Hz, 1H), 3.87–3.65 (m, 2H), 2.67–2.53 (m, 1H), 2.50–2.36 (m, 1H), 1.91 (br s, 1H), 1.75 (br s, 1H). HRMS (ESI) m/z: $[M+Na]^+$ Calcd for $C_{23}H_{18}F_3N_3O_3Na^+$:464.1192; Found: 464.1193.

Additional information on the chemical synthesis and the analysis of the target compound is available via the Chemotion repository: https://dx.doi.org/10.14272/reaction/SA-FUHFF-UHFFFADPSC-WEQVDYVYYA-UHFFFADPSC-NUHFF-NUHFF-NUHFF-ZZZ.

Deposition Number(s) 2215510 (for **IC9O-COOMe**) and 2217275 (for **7**) contain(s) the supplementary crystallographic data for this paper. These data are provided free of charge by the joint Cambridge Crystallographic Data Centre and Fachinformationszentrum Karlsruhe Access Structures service.

All synthetic details, original NMR, and MS data were submitted to the repository Chemotion (http://www.chemotion-repository.net/). All DOIs minted for the data are linked to the specific experiments in the Supporting Information, and a summary of all new data obtained in this study can be gained with the collection DOIs: https://dx.doi.org/10.14272/collection/AAL_2022-12-18_2 and https://dx.doi.org/10.14272/collection/AAL_2023-05-23.

Acknowledgements

This work represents an integration of diverse projects funded by the Russian Foundation for Basic Research (NAD grant 20-03-00117 investigations in cycloalkynes synthesis and SPAAC reactivity) and the Russian Science Foundation (IAB grant 21-13-00218 quantum mechanical computations and study of photophysical properties). The research was carried out using the SPbU Resource Centres equipment: Magnetic Resonance Research Centre, Chemical Analysis and Materials Research Centre, Centre for X-ray Diffraction Studies, Centre for Optical and Laser Materials Research, and Computer Centre. Alexander Y. Ivanov (SPbU) and Sergey N. Smirnov (SPbU) are thanked for the NMR measurements; Oussama Abdelhamid Mammeri (SPbU) and Alexander Gorbunov (Research Institute of Hygiene, Occupational Pathology and Human Ecology) are thanked for HR MS measurements. Dr. Nicole Jung (KIT) is grateful for her help with the Chemotion deposit. We are thankful to Emma Puttock (KIT) for their valuable repository comments and remarks. Open Access funding enabled and organized by Projekt DEAL.

Conflict of Interests

The authors declare no conflict of interest.

Data Availability Statement

The data that support the findings of this study are available in the supplementary material of this article.

Keywords: ab initio calculations · azide · click chemistry · cycloalkyne · fluorescence · SPAAC · triazole

[1] E. M. Sletten, C. R. Bertozzi, *Angew. Chem. Int. Ed.* **2009**, *48*, 6974–6998.
[2] C. S. McKay, M. G. Finn, *Chem. Biol.* **2014**, *21*, 1075–1101.
[3] B. Liu Kenry, *Trends Chem.* **2019**, *1*, 763–778.
[4] S. S. Nguyen, J. A. Prescher, *Nat. Chem. Rev.* **2020**, *4*, 476–489.
[5] Y. Li, H. Fu, *ChemistryOpen* **2020**, *9*, 835–853.
[6] S. L. Scinto, D. A. Bilodeau, R. Hincapie, W. Lee, S. S. Nguyen, M. Xu, C. W. am Ende, M. G. Finn, K. Lang, Q. Lin, J. P. Pezacki, J. A. Prescher, M. S. Robillard, J. M. Fox, *Nat. Rev. Methods Prim.* **2021**, *1*, 30.
[7] T. Deb, J. Tu, R. M. Franzini, *Chem. Rev.* **2021**, *121*, 6850–6914.
[8] Y. Takayama, K. Kusamori, M. Nishikawa, *Molecules* **2019**, *24*, 172.
[9] V. Rigolot, C. Biot, C. Lion, *Angew. Chem. Int. Ed.* **2021**, *60*, 23084–23105.
[10] http://www.nobelprize.org/uploads/2022/10/press-chemistryprize2022-2.pdf n.d.
[11] N. J. Agard, J. A. Prescher, C. R. Bertozzi, *J. Am. Chem. Soc.* **2004**, *126*, 15046-15047.
[12] E. M. Sletten, C. R. Bertozzi, *Acc. Chem. Res.* **2011**, *44*, 666–676.
[13] E. Kim, H. Koo, *Chem. Sci.* **2019**, *10*, 7835–7851.
[14] C. J. Pickens, S. N. Johnson, M. M. Pressnall, M. A. Leon, C. J. Berkland, *Bioconjugate Chem.* **2018**, *29*, 686–701.
[15] J. Kaur, M. Saxena, N. Rishi, *Bioconjugate Chem.* **2021**, *32*, 1455–1471.
[16] M. F. Debets, C. W. J. van der Doelen, F. P. J. T. Rutjes, F. L. van Delft, *ChemBioChem* **2010**, *11*, 1168–1184.

[17] J. Dommerholt, F. P. J. T. Rutjes, F. L. van Delft, *Top. Curr. Chem.* **2016**, *374*, 16.
[18] T. Harris, I. V. Alabugin, *Mendeleev Commun.* **2019**, *29*, 237–248.
[19] J. H. Rothman, *ACS Omega* **2022**, *7*, 9053–9060.
[20] J. Weterings, C. J. F. Rijcken, H. Veldhuis, T. Meulemans, D. Hadavi, M. Timmers, M. Honing, H. Ippel, R. M. J. Liskamp, *Chem. Sci.* **2020**, *11*, 9011–9016.
[21] Y. Hu, J. M. Roberts, H. R. Kilgore, A. S. Mat Lani, R. T. Raines, J. M. Schomaker, *J. Am. Chem. Soc.* **2020**, *142*, 18826–18835.
[22] J. M. Dones, N. S. Abularrage, N. Khanal, B. Gold, R. T. Raines, *J. Am. Chem. Soc.* **2021**, *143*, 9489–9497.
[23] D. M. Monzón, J. M. Betancort, T. Martín, M. Á. Ramírez, V. S. Martín, D. Díaz Díaz, *Molecules* **2021**, *26*, 1629.
[24] M. Li, X. Ma, C. J. Molnar, S. Wang, Z. Wu, V. V. Popik, Z. Li, *Bioconjugate Chem.* **2022**, *33*, 2088–2096.
[25] M. J. Holzmann, N. Khanal, P. Yamanushkin, B. Gold, *Org. Lett.* **2023**, *25*, 309–313.
[26] J. Brauer, M. Mötzing, C. Gröst, R. Hoffmann, T. Berg, *Chem. A Eur. J.* **2022**, *28*, e202202259.
[27] Y. Sakata, R. Nabekura, Y. Hazama, M. Hanya, T. Nishiyama, I. Kii, T. Hosoya, *Org. Lett.* **2023**, *25*, 1051–1055.
[28] X. Ren, A. H. El-Sagheer, T. Brown, *Nucleic Acids Res.* **2016**, *44*, e79-e79.
[29] J. C. Jewett, C. R. Bertozzi, *Org. Lett.* **2011**, *13*, 5937–5939.
[30] J.-J. Shie, Y.-C. Liu, J.-C. Hsiao, J.-M. Fang, C.-H. Wong, *Chem. Commun.* **2017**, *53*, 1490–1493.
[31] F. Friscourt, C. J. Fahrni, G.-J. Boons, *J. Am. Chem. Soc.* **2012**, *134*, 18809–18815.
[32] V. Terzic, G. Pousse, R. Méallet-Renault, P. Grellier, J. Dubois, *J. Org. Chem.* **2019**, *84*, 8542–8551.
[33] X. Sun, T. Liu, J. Sun, X. Wang, *RSC Adv.* **2020**, *10*, 10826–10847.
[34] A. Pereira, S. Martins, A. Teresa Caldeira, *in Phytochem. Hum. Heal.*, IntechOpen, **2020**, pp. 1–20.
[35] M. Okazaki, N. Yagi, Y. Wakizaka, *J. Synth. Org. Chem. Japan* **1968**, *26*, 155–160.
[36] J. Amemura-Maekawa, Y. Hayakawa, H. Sugie, A. Moribayashi, F. Kura, B. Chang, A. Wada, H. Watanabe, *Biochem. Biophys. Res. Commun.* **2004**, *323*, 954–959.
[37] S. N. Karuk Elmas, Z. E. Dincer, A. S. Erturk, A. Bostanci, A. Karagoz, M. Koca, G. Sadi, I. Yilmaz, *Spectrochim. Acta Part A* **2020**, *224*, 117402.
[38] V. Pirovano, M. Marchetti, J. Carbonaro, E. Brambilla, E. Rossi, L. Ronda, G. Abbiati, *Dyes Pigm.* **2020**, *173*, 107917.
[39] S. Pathak, D. Das, A. Kundu, S. Maity, N. Guchhait, A. Pramanik, *RSC Adv.* **2015**, *5*, 17308–17318.
[40] N. A. Danilkina, A. I. Govdi, A. F. Khlebnikov, A. O. Tikhomirov, V. V. Sharoyko, A. A. Shtyrov, M. N. Ryazantsev, S. Bräse, I. A. Balova, *J. Am. Chem. Soc.* **2021**, *143*, 16519–16537.
[41] A. S. Klymchenko, *Acc. Chem. Res.* **2017**, *50*, 366–375.
[42] G. Li Manni, R. K. Carlson, S. Luo, D. Ma, J. Olsen, D. G. Truhlar, L. Gagliardi, *J. Chem. Theory Comput.* **2014**, *10*, 3669–3680.
[43] S. Breda, I. Reva, L. Lapinski, R. Fausto, *Phys. Chem. Chem. Phys.* **2004**, *6*, 929–937.
[44] J. L. Menke, R. J. McMahon, *Can. J. Chem.* **2011**, *89*, 186–194.
[45] M. A. Kinder, J. Kopf, P. Margaretha, *Tetrahedron* **2000**, *56*, 6763–6767.
[46] M. S. Weerasinghe, S. T. Karlson, Y. Lu, K. A. Wheeler, *Cryst. Growth Des.* **2016**, *16*, 1781–1785.
[47] K. Sonogashira, Y. Tohda, N. Hagihara, *Tetrahedron Lett.* **1975**, *16*, 4467–4470.
[48] I. Kanwal, A. Mujahid, N. Rasool, K. Rizwan, A. Malik, G. Ahmad, S. A. A. Shah, U. Rashid, N. M. Nasir, *Catalysts* **2020**, *10*, 443.
[49] D. Yue, R. C. Larock, *J. Org. Chem.* **2002**, *67*, 1905–1909.
[50] T. Aggarwal, S. Kumar, A. K. Verma, *Org. Biomol. Chem.* **2016**, *14*, 7639–7653.
[51] K. M. Nicholas, R. Pettit, *J. Organomet. Chem.* **1972**, *44*, C21-C24.
[52] P. Röse, G. Hilt, *Synthesis (Stuttg).* **2015**, *48*, 463–492.
[53] N. Kann, *Curr. Org. Chem.* **2012**, *16*, 322–334.
[54] B. J. Teobald, *Tetrahedron* **2002**, *58*, 4133–4170.
[55] R. Ni, N. Mitsuda, T. Kashiwagi, K. Igawa, K. Tomooka, *Angew. Chem. Int. Ed.* **2015**, *54*, 1190–1194.
[56] K. Igawa, S. Aoyama, Y. Kawasaki, T. Kashiwagi, Y. Seto, R. Ni, N. Mitsuda, K. Tomooka, *Synlett* **2017**, *28*, 2110–2114.
[57] K. Kaneda, R. Naruse, S. Yamamoto, *Org. Lett.* **2017**, *19*, 1096–1099.
[58] T. Hagendorn, S. Bräse, *RSC Adv.* **2014**, *4*, 15493–15495.
[59] A. B. Neef, N. W. Luedtke, *ChemBioChem* **2014**, *15*, 789–793.
[60] N. E. Mbua, J. Guo, M. A. Wolfert, R. Steet, G.-J. Boons, *ChemBioChem* **2011**, *12*, 1912–1921.
[61] S. Dhar, D. K. Rana, S. Singha Roy, S. Roy, S. Bhattacharya, S. C. Bhattacharya, *J. Lumin.* **2012**, *132*, 957–964.
[62] S. Drouet, C. O. Paul-Roth, V. Fattori, M. Cocchi, J. A. G. Williams, *New J. Chem.* **2011**, *35*, 438–444.
[63] O. Exner, S. Böhm, *New J. Chem.* **2008**, *32*, 1449.

Manuscript received: February 18, 2023
Accepted manuscript online: June 9, 2023
Version of record online: ■■, ■■

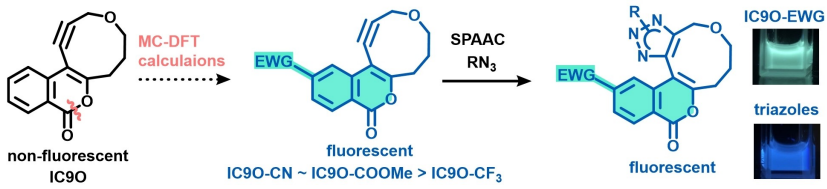

Fluorescent pairs of isocoumarin-fused cycloalkynes **IC9O-COOMe** and **IC9O-CN**/1,2,3-triazoles were developed. The basis for creating **IC9O-EWG** is understanding the reason for the S1 state deactivation mechanism for their non-fluorescent analog **IC9O** using multi-configurational ab initio and DFT methodologies and eliminating this deactivation pathway through rational design.

A. A. Vidyakina, A. A. Shtyrov, Dr. M. N. Ryazantsev, Prof. Dr. A. F. Khlebnikov, Dr. I. E. Kolesnikov, Dr. V. V. Sharoyko, Dr. D.'y. V. Spiridonova, Prof. Dr. I. A. Balova, Prof. Dr. S. Bräse, Dr. N. A. Danilkina**

1 – 14

Development of Fluorescent Isocoumarin-Fused Oxacyclononyne – 1,2,3-Triazole Pairs